ISSN 0036-0244, Russian Journal of Physical Chemistry A, 2009, Vol. 83, No. 9, pp. 1526–1530. © Pleiades Publishing, Ltd., 2009.

STRUCTURE OF MATTER AND QUANTUM CHEMISTRY

Large Deviation Spectra of Chaotic Time Series from Bray–Liebhafsky Reaction*

A. Z. Ivanović[a], Ž. D. Čupić[a], Lj. Z. Kolar-Anić[b], M. M. Janković[c], and S. R. Anić[b]

[a] *ICh TM—University of Belgrade, Department of Catalysis and Chemical Engineering, Serbia*

[b] *Faculty of Physical Chemistry, University of Belgrade, Serbia*

[c] *Institute for Nuclear Science, Belgrade, Serbia*

e-mail: ana.ivanovic@nanosys.ihtm.bg.ac.rs

Abstract—We applied multifractal analysis on time series obtained by deterministic simulation of the Bray–Liebhafsky oscillatory reaction. Large deviation spectrum was used to represent multifractal properties of the attractor. We obtained spectrums with two peaks, one in region of low and the other in region of high values of Hölder exponent. Their intensity depends on flow rate. The method developed on the results from numerical simulations is tested on the experimental record from the same reaction system and multifractality of the time series is confirmed.

DOI: 10.1134/S0036024409090192

INTRODUCTION

The Bray–Liebhafsky (BL) reaction is the decomposition of hydrogen peroxide into the water and oxygen in the presence of iodate and hydrogen ions:

$$2H_2O_2 \xrightarrow{H^+, IO_3^-} O_2 + 2H_2O. \qquad (D)$$

This apparently simple reaction is a highly nonlinear process that comprises a complex homogeneous catalytic oscillatory evolution involving numerous iodine intermediates [1, 2].

Oscillatory dynamics of the BL reaction is best described by the model consisted of eight reactions:

$$IO_3^- + I^- + 2H^+ \rightleftharpoons HIO + HIO_2, \qquad (R1), (R\text{-}1)$$

$$HIO_2 + I^- + H^+ \longrightarrow I_2O + H_2O, \qquad (R2)$$

$$I_2O + H_2O \rightleftharpoons 2HIO, \qquad (R3), (R\text{-}3)$$

$$HIO + I^- + H^+ \rightleftharpoons I_2 + H_2O, \qquad (R4), (R\text{-}4)$$

$$HIO + H_2O_2 \longrightarrow I^- + H^+ + O_2 + H_2O, \qquad (R5)$$

$$I_2O + H_2O_2 \longrightarrow HIO + HIO_2, \qquad (R6)$$

$$HIO_2 + H_2O_2 \longrightarrow IO_3^- + H^+ + H_2O, \qquad (R7)$$

$$IO_3^- + H^+ + H_2O_2 \longrightarrow HIO_2 + O_2 + H_2O. \qquad (R8)$$

Three of them are reversible. Nevertheless, for numerical simulations of the system behavior in the continuous stirred tank reactor (CSTR) the reactions due to flow of hydrogen peroxide through the system and outflow of all species from the reaction vessel must be added. The resulting model for the BL reaction in the CSTR and rate constants are given in [3]. Different variants of the model are additionally elaborated in [4, 5].

With increasing flow rate j_0, in numerical simulations based on this model, various simple, complex, and chaotic oscillations were observed [6].

For complex oscillation description, many different methods were applied on BL reaction such as firing numbers, power spectra and Poincaré section [6]. The appearance of deterministic chaos in the experimental and simulated BL reaction was also confirmed and proven by the determination of positive values of the maximal Lyapunov exponents for the sequences of flow rate values as the control parameter [3]. Although typical for chaos quantification, fractal properties of the BL reaction were not tested ever before.

An object (function, set of phase space points or simply data) is usually referred to as fractal if its graph displays such characteristics as (local) selfsimilarity, irregularity, fine structure, and fractional dimension [7]. Dissipative dynamical systems that exhibit chaotic behavior, often has strange attractor in phase space [8]. Strange attractors are typically characterized by fractal dimension D [9] which is smaller than the number of degrees of freedom F ($D < F$). Moreover, different parts of an attractor may be characterized by different value of the fractal dimension. In such situation, a single value of some fractal dimension is not sufficient to characterize the attractor adequately. For example, two quite different attractors might have the same correlation dimension, but they still could differ widely in their "appearance." One can visualize this multifractal object as a collection of overlapping fractal objects, each with its own fractal dimension [10].

Multifractal techniques and notions are increasingly widely recognized as the most appropriate and

*The article is published in the original.

straightforward framework to analyze scale dependency of the data, but also their extreme variability over a wide range of scales [11]. However, fractal dimension is measure of global scaling property but multifractality depends on local scaling properties of the object, and therefore, obviously, there is a need for some other quantity to qualify the system. Hence, the basic numerical expression used in the multifractal analysis is so-called Hölder exponent, α [12]. The Hölder exponent of a data is a local characteristic value calculated at each point in time series. It reflects the decay rate of the amplitude of the function fluctuation μ, in the neighborhood of the point j as the size ε of the neighborhood shrinks to zero:

$$\mu_j(\varepsilon) \propto \varepsilon^{\alpha_j}. \quad (1)$$

A highly irregular point (or singularity) in a data is characterized by a lower value of Hölder exponent and a smoother portion of a data will have a higher value of Hölder exponent. A time series may have different Hölder exponents at different points due to a variation in the local degree of irregularity (or singularity).

The number of intervals $N(\alpha)$ where the time series has Hölder exponents between α and $\alpha + d\alpha$ scale as [13]

$$N(\alpha) \sim \varepsilon^{-f(\alpha)}, \quad (2)$$

where $f(\alpha)$ can be considered as the generalized fractal dimension of the set of boxes with singularities α. The multifractal spectrum is graph, where abscissa represents the Hölder exponent in the signal and the ordinate is the generalized fractal dimension $f(\alpha)$ which measures the extent by which a given singularity is encountered. Multifractal spectrum can be evaluated directly from equations given above (1) and (2) (and actually it is calculated this way in Large deviation spectrum calculations) but it is hard task. More usual and easier procedure for multifracatal spectrum analysis is indirect one, based on generalization of the measure of signal variation to so called partition sum:

$$Z(q, \varepsilon) = \sum_{i=1}^{N(\varepsilon)} \mu_i^q, \quad (3)$$

where q is a real parameter that indicates the order of the moment of the measure. The parameter q can be considered as a powerful microscope, able to enhance the smallest differences of two very similar maps [14]. Furthermore, q represents a selective parameter: high values of q enhance boxes with relatively high values for $\mu_j(\varepsilon)$; while low values of q favor boxes with relatively low values of $\mu_j(\varepsilon)$. Partition sum Z scales as

$$Z(q, \varepsilon) \sim \varepsilon^{\tau(q)}, \quad (4)$$

where $\tau(q)$ is the correlation exponent of the q-th order moment defined as [15]

$$\tau(q) = (q-1)D_q \quad (5)$$

and D_q is generalized dimensions that can be calculated from [16]

$$D_q = \lim_{\varepsilon \to 0}\left(\frac{1}{q-1}\frac{\log Z(q, \varepsilon)}{\log(\varepsilon)}\right). \quad (6)$$

The generalized dimension D_q is a monotonic decreasing function for all real values of q within the domain $[-\infty, +\infty]$.

The connection between the power exponents $f(\alpha)$, which can be considered as the generalized fractal dimension of the set of boxes with singularities α, and $\tau(q)$ is made via the Legendre transformation [13, 15]:

$$f_L(\alpha(q)) = q\alpha(q) - \tau(q) \quad (7)$$

and

$$\alpha(q) = d\tau(q)/dq. \quad (8)$$

Therefore, the multifractal spectrum $f(\alpha)$ is usually obtained from evaluation of generalized dimension D_q and subsequent Legendre transformation of $\tau(q)$ using Eqs. (7) and (8). The $f_L(\alpha)$ is a concave downward function with a maximum at $q = 0$ and it describes properties of multifractal. Single humped function $f(\alpha)$ obtained for multifractal spectrum is very useful and easily discussed in terms of capacity, information, and correlation dimension. Therefore it is widely applied [17–19]. However, its shape is mainly consequence of the applied Legendre transform. Actual distribution of the points with various Hölder exponents could be obtained through the Large deviation spectrum.

The large deviation spectrum $f_G(\alpha)$ which is based on the Cramér theory of large Deviations [15, 20] is, in accordance with Eqs. (1) and (2), defined as:

$$f_G(\alpha) = \lim_{\varepsilon \to 0} \lim_{n \to \infty} \frac{\ln N_\varepsilon^n(\alpha)}{-\ln \delta_n}. \quad (9)$$

The function $f_G(\alpha)$ reflects the exponentially decreasing rate of $N_\varepsilon^n(\alpha)$ which is the number of intervals having a Hölder exponent, α_i^n, close to a Hölder exponent α up to a precision δ when the resolution n (the number of intervals in the α space) approaches ∞. The $f_G(\alpha)$ yields the large deviations from the "most frequent" singularity exponent and thus displays information about the occurrence of rare events such as bursts (small α).

For detailed comparison of various chaotic states, multifractal analysis is used here, rather than local fractal dimension evaluation, since it may yield additional insight into the complex nature of the chaotic dynamical state [10]. The large deviation spectrum yields information about the statistical behavior of the probability of finding a point with a given Hölder exponent in the signal under changes of resolution [17].

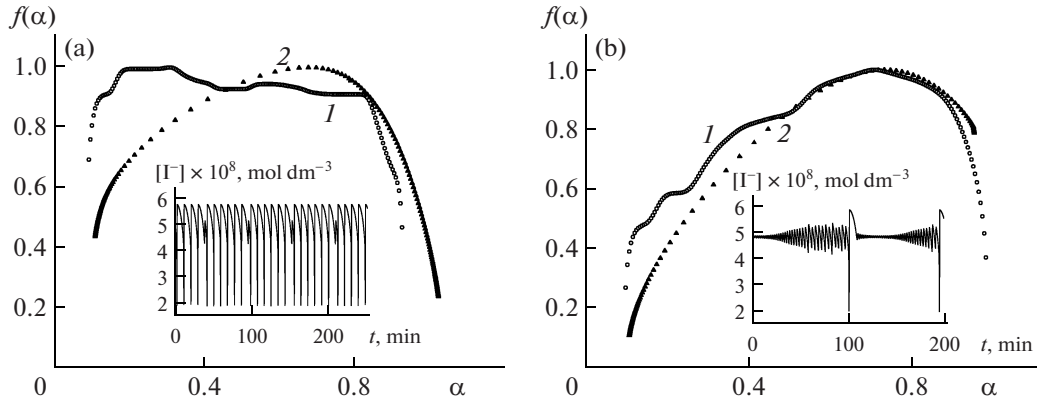

Fig. 1. (*1*) Large deviation and (*2*) Legendre spectrum for the time series from the simulations in the function of the flow rate as a control parameter: (a) 4.82592×10^{-3}, (b) 5.0812×10^{-3} min^{-1}; α is Hölder exponent.

METHODS

Deterministic simulations were performed using the MATLAB program package using the ode15s solver. For the numerical calculation of the large deviation spectrum, the FRACLAB toolbox has been used [21].

The Bray–Liebhafsky oscillatory reaction, was conducted in CSTR. The procedure is described in more detail earlier [3]. The initial experimental conditions were: $[KIO_3]_0 = 5.9 \times 10^{-2}$ mol dm^{-3}, $[H_2SO_4]_0 = 5.5 \times 10^{-2}$ mol dm^{-3}, $[H_2O_2]_0 = 2.0 \times 10^{-1}$ mol dm^{-3}, $T = 48.6$°C. The specific flow rate was 5.03×10^{-3} min^{-1}. Temporal evolution of the BL system was monitored potentiometrically by Pt (Metrohm-6.0301.100) electrode versus a double junction Ag/AgCl (Metrohm-6.0726.100) electrode as the reference.

RESULTS AND DISCUSSION

Generally, multifractal analysis is the method for examination of time series with highly irregular oscillation periods and their amplitudes. The BL reaction in chaotic regime also have the irregular time series, but with two types of oscillations with significantly different periods and amplitudes. Moreover, the amplitudes of large oscillations are almost same whereas the amplitudes of small oscillations are different between themselves.

The model of the BL reaction system in chaotic regime appears to be very sensitive to changes of the control parameter (similar to the experimental one) and complex dynamic states appear in a very narrow region of flow rates, j_0. In much wider oscillatory region, for low values of j_0 only large amplitude relaxation oscillations are observed. Between complex dynamic states and bifurcation to steady state at high j_0, there is a region of j_0 values where only small-amplitude oscillations are found. The mixed-mode oscillations consist of these two kind of simple sustained oscillations (large-amplitude relaxation and small-amplitude, nearly sinusoidal ones) involved one into the other. The mixed-mode dynamic states appear in the form evolving with flow rate from X^1 to 1^Y, which denote the number of large and small amplitude oscillations in one sequence, respectively. Among them, windows of more complex dynamic states such as the mixture of regular mixed-mode oscillations, period doubling, and deterministic chaos are found.

The insets at the Fig. 1 illustrate two kinds of complex oscillations with dominating X^1 (Fig. 1a) and 1^Y (Fig. 1b) forms of dynamics. We applied both, the Legendre spectrum and the large deviation spectrum on these chaotic time series and results are shown in Fig. 1. Well defined multifractal type spectra were obtained in both cases. By application of large deviation spectrum on these chaotic time series obtained at different flow rates we have found one kind of bimodal distribution which depends on fraction of large and small amplitude oscillations. Legendre spectrum which is more usual in multifractal analysis shows here skewed form with maximum near to the second peak of the large deviation spectrum. Lower Hölder exponents wing of the large deviation spectrum is not covered with Legendre spectrum, indicating significant information lost, which is more pronounced for lower values of the flow rate, where the dynamic state is typically of the X^1 form. Therefore, we decided to use the large deviation spectrum in the multifractal analysis of time series from numerical simulations of the BL reaction.

At lower flow rates ($j_0 = 4.82592 \times 10^{-3}$ min^{-1}) large deviation spectrum gives higher contribution of lower Hölder exponents that correspond to situation when fraction of large amplitude oscillations is higher. The situation is opposite at higher flow rates ($j_0 = 5.0812 \times 10^{-3}$ min^{-1}). The large deviation spectrum is analyzed for several values of the flow rate as the control parameter in simulation, keeping all other parameters constant. The intensities of the two peaks, corresponding to the low and high Hölder exponent values, are presented in Fig. 2, in function of the flow rate.

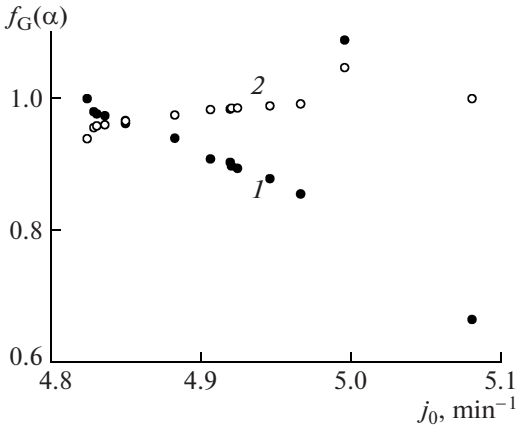

Fig. 2. Intensity of two peaks (*1*) lower α, (*2*) higher α in the large deviation spectrum in a function of the flow rate.

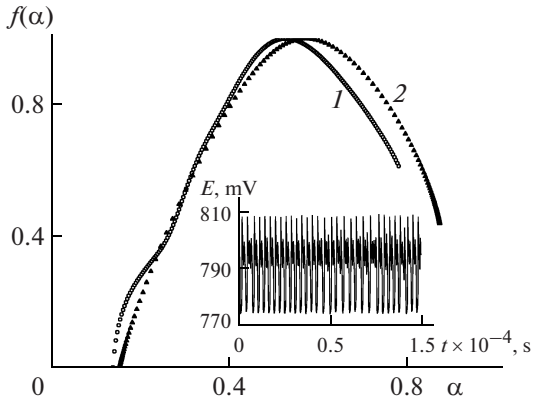

Fig. 3. (*1*) Large deviation and (*2*) Legendre spectrum for the selected experimental time series: the initial experimental conditions were: $[KIO_3]_0 = 5.9 \times 10^{-2}$ mol dm^{-3}, $[H_2SO_4]_0 = 5.5 \times 10^{-2}$ mol dm^{-3}, $[H_2O_2]_0 = 0.2$ mol dm^{-3}, $T = 48.6$°C, flow rate 5.03×10^{-3} min^{-1}.

From Fig. 2 we can see that contribution of lower exponent peak decreases, while higher one increases, with increasing flow rate. It is similar to the pattern followed by the fractions of large and small oscillations, respectively. It can be concluded that, from the statistical point of view, given by large deviation spectrum analysis, the level of singularity in the analyzed numerical time series, continuously decreases with increasing flow rate. Since the large oscillation fraction also decreases in the same direction, it can be connected with measured irregularities in time series. Roughly speaking, in our case, large oscillations correspond to the large fluctuations and therefore to the large concentration of the measure μ and therefore to large q values and small Hölder exponent values.

Since the applicability of the large deviation spectrum is approved in the numerical simulations of the BL reaction, the same method is also used here to test the data obtained from the experimental record of the Pt electrode potentiometric measurements in BL reaction under CSTR conditions. Results for both Legendre spectrum and the large deviation spectrum of the sample experimental time series are presented in Fig. 3.

The same type of spectra is obtained for the experimental record, as previously for the numerical simulations. Relatively good agreement between two spectra is typical for the form of the X^1 dynamical state. The shape of the spectra indicates multifractal nature of the time series and of corresponding attractor in phase space. The maximum of both spectra almost coincide in this case, and it takes Hölder exponent value significantly lower then one, demonstrating highly irregular, chaotic behavior of the BL reaction in CSTR.

CONCLUSIONS

Time series were obtained by numerical integration of the ordinary differential equations for the Bray–Liebhafsky oscillatory reaction model in the CSTR reactor under the conditions of the deterministic chaos and mixed mode periodic oscillations. The applicability of the multifractal analysis in comparison of various chaotic states was demonstrated. For the low flow rate value, smaller Hölder exponents dominate, indicating appearance of signal fractality, while for the increased flow rate values higher Hölder exponents are more pronounced. Established multifractal analysis method is also successfully applied on the experimentally recorded time series from the BL reaction in CSTR and multifractal nature of the record is confirmed.

ACKNOWLEDGMENTS

The authors thank the partial support of the Fund for Science and Technologies and Development of Serbia (Projects 142019 and 142025).

REFERENCES

1. W. C. Bray, J. Am. Chem. Soc. **43**, 1262 (1921).
2. W. C. Bray and H. A. Liebhafsky, J. Am. Chem. Soc. **53**, 38 (1931).
3. A. Z. Ivanović, Ž. D. Čupić, M. M. Janković, Lj. Z. Kolar-Anić, and S. R. Anić, Phys. Chem. Chem. Phys. **10**, 5848 (2008).
4. Lj. Kolar-Anić, N. Vukelić, D. Mišljenović, and S. Anić, J. Serb. Chem. Soc. **60**, 1005 (1995).
5. Lj. Kolar-Anić, Ž. Čupić, S. Anić, and G. Schmitz, J. Chem. Soc., Faraday Trans. **93**, 2147 (1997).
6. G. Schmitz, Lj. Kolar-Anić, S. Anić, T. Grozdić, and V. Vukojević, J. Phys. Chem. A **110**, 10361 (2006).

7. K. Falconer, *Fractal Geometry: Mathematical Foundations and Applications* (Wiley, New York, 1990).
8. D. Rulle and F. Takens, Commun. Math. Phys. **20**, 167 (1971).
9. B. B. Mandelbrot, *Fractals-form, Chance and Dimension* (Freeman, San Francisko, 1977).
10. R. C. Hilborn, *Chaos and Nonlinear Dynamics*, 2nd ed. (Oxford Univ., Oxford, 2000).
11. D. Schertzer and S. Lovejoy, in *Proc. of the EGS Richardson AGU Chapman NVAG3 Conference: Nonlinear Variability in Geophysics: Scaling and Multifractal Processes*, Nonlinear Processes in Geophys., Eur. Geophys. Soc. **1**, 77 (1994).
12. L. J. Véhel and R. Vojak, Adv. Appl. Mat. **20**, 1 (1998).
13. A. Chhabra and R. Jensen, Phys. Rev. Lett. **62**, 1327 (1989).
14. J. M. Diego, E. Martinez-Gonzales, J. L. Sanz, S. Mollerach, and V. J. Mart, Mon. Not. R. Astron. Soc. **306**, 427 (1999).
15. T. Halsey, M. Jensen, L. Kadanoff, I. Procaccia, and B. Shraiman, Phys. Rev. A **33**, 1141 (1986).
16. H. Hentschel and I. Procaccia, Physica D **8**, 435 (1983).
17. M. Meyer and O. Stiedl, Eur. J. Appl. Physiol. **90**, 305 (2003).
18. S. Peng-Jian and S. Jin-Sheng, Chin. Phys. Soc. **16**, 365 (2007).
19. L. Telesca, M. Balasco, G. Colangelo, V. Lapenna, and M. Macchiato, Phys. Chem. Earth **29**, 295 (2004).
20. R. Holley and E. Waymire, Ann. Appl. Prob. **2**, 819 (1992).
21. http://apis.saclay.inria.fr/FracLab/download.html.